Let's All Pull Together: Principles for Sharing Large Loads in Microrobot Teams

David L. Christensen, Srinivasan A. Suresh, Katie Hahm, and Mark R. Cutkosky

***Abstract*— We present a simple statistical model to predict the maximum pulling force available from robot teams. The expected performance is a function of interactions between each robot and the ground (e.g. whether running or walking). We confirm the model with experiments involving impulsive bristlebots, small walking and running hexapods, and 17 gram µTugs that employ adhesion instead of friction. With attention to load sharing, each µTug can operate at its individual limit so that a team of six pulls with forces exceeding 200 N.**

I. Introduction

Among the potentially useful capabilities of miniature robots is the ability to form teams that can exert forces and manipulate objects much larger than themselves. In this regard, the collective actions of leaf cutter ants are a common source of inspiration [1]–[3]. However, with a few exceptions, microrobots can exert only small forces individually, and the ability to exert large forces in teams is comparatively unexplored.

In this paper we examine the characteristics of small robots that make them inherently more or less suited to pulling heavy loads. An interesting result is that optimizing a single robot to exert the maximum peak force when pushing or pulling an object may render it less suitable for working in a team. Equally important are the characteristics of the interaction between each robot's feet and the ground. A reliance on Coulomb friction severely limits the force that each robot can exert and correspondingly limits the capabilities of the team.

We explore these issues in three broadly defined classes of mobile robots: *impulsive*, *smooth-gaited*, and *winching*. The winching robots are based on µTugs [4], which use controllable adhesion instead of friction to interact with the ground. Each µTug can pull a large load in proportion to its weight and, with some attention to configuration and control, a team of µTugs can achieve a nearly proportional increase in load carrying ability with increasing numbers of robots. For example, six µTugs, each with a mass of 17 g, can pull a 1800 kg automobile and driver on polished concrete (Fig. 1).

The paper first introduces the concepts of smooth versus impulsive gaits and then introduces a statistical model to predict how effectively their forces against the ground will add. The model requires no particular assumptions about the details of robot/ground interactions, inertial dynamics, friction, etc. The results of the statistical prediction are compared with experiments and logical extensions of the model are explored to give insights into load sharing mechanics within a team.

All Authors are with Mechanical Engineering Dept., Stanford University. BDML at Center for Design Research, 424 Panama Mall, Bldg. 560, Stanford, CA 94305-2232. Email: davidc10@stanford.edu

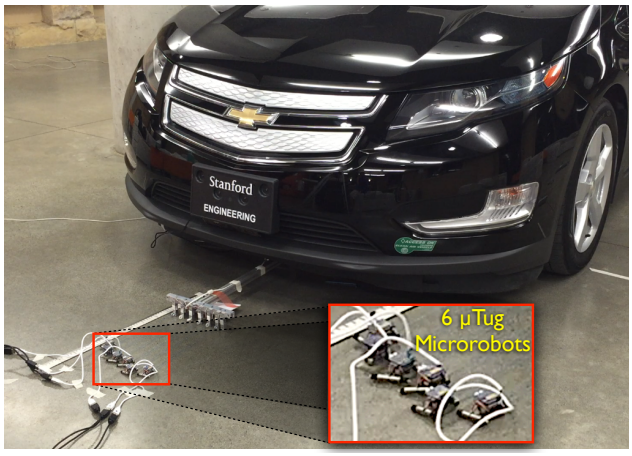

Fig. 1. A 1800 kg automobile is pulled by a team of 6 µTug robots on a concrete floor with load sharing for a combined force of 200 N.

A. Related work

While there are many interesting examples of terrestrial microrobots [5]–[7], in most cases, these rely on friction between the robot and the ground. As noted in [8], it is often desirable to operate in a regime where such robots can exploit the difference between static and dynamic coefficients of friction. Alternatively, microrobots can utilize anisotropic friction or adhesion with the ground or on vertical surfaces [4], [7], [9]–[13].

There are several examples of prior work on cooperating teams of robots (e.g., [14]–[16]) but most of these focus on design of systems for individual control of externally actuated robots, cost reduction for feasible manufacturing, or strategies for cooperation.

II. Mechanics of Microrobot Locomotion

We begin with a discussion of the mechanics of gait and force generation for the three broad classes of robots previously mentioned. Let t_p be the stride period of the robot's gait, and t_c be the duration of contact between the foot and the ground in a stride period, during which the robot exerts a horizontal force f_c. We allow the foot contact time to be in the range $0 < t_\mathrm{c} \leq t_\mathrm{p}$. The ratio t_c/t_p allows us to distinguish among *impulsive*, *smooth* and *winch* gaits.

A. Impulsive gait

Running robots like the MIT Cheetah [17] are intentionally impulsive. The choice of a galloping gait with just one, or

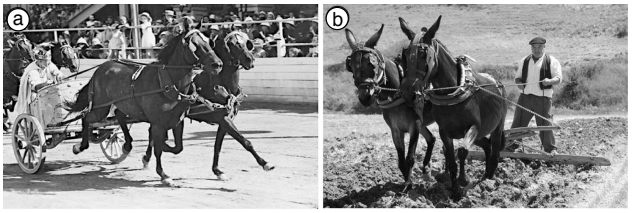

Fig. 2. (a) Horses gallop with a chariot. Force is applied in bursts as feet strike the ground. The gait has an airborne phase, so a consistent pulling force is impossible. (b) A team of mules pulls a plow by walking with at least two feet on the ground at any time, providing a consistent force [21].

even zero, feet in contact with the ground at each instant gives the legs maximum time to recycle for the next stride. A characteristic of impulsive locomotion is that $t_c \ll t_p$. In the case of the horses and chariot in Fig. 2a, momentum is large and carries the load forward, sustained by a steady sequence of impulses from the feet.

At the opposite extreme, tiny "bristlebots" are also impulsive. Locomotion proceeds by a series of many extremely small and brief impulsive interactions with the ground. As noted in [18] this yields controllability benefits, especially for systems prone to "stiction."

An advantage of such gaits for small robots is that they do not require a complex power transmission system to convert between a small, high speed actuator to comparatively long strides and high forces. Instead, one can use an oscillatory actuator–for example, a small motor and eccentric mass, or a piezoelectric actuator–that operates at high speed. The inertial forces produced by such an actuator, combined with a significant difference between the static and dynamic coefficient of friction, are sufficient to propel the robot.

An additional useful characteristic of impulsive locomotion is that the peak force associated with each foot/ground contact can be quite large, exceeding the weight of the robot [19]. Hence a small robot employing impulsive locomotion can slowly move a large object by repeatedly "hammering" at it. However, as we will see in the next section, this characteristic makes impulsive robots inherently more difficult to harness in teams.

B. Smooth gait

Fig. 2b illustrates two mules pulling a plow with a smooth gait. The resistance of the plow precludes any coasting between footfalls. The mules instead use a smooth walking gait, and the force they apply to the plow is relatively constant. Many robots as they transition from running to walking will apply a more uniform horizontal force, provided that the legs have a sufficiently long stride length that t_c is a large fraction of t_p. Interestingly, small insects that run with a "groucho gait" (i.e., with a bouncing periodic motion but no airborne phase) can, due to their long limbs, produce an oscillating but not impulsive force profile [20]. Of course, wheeled and tracked vehicles also exhibit a smooth gait.

C. Winch gait

The winch gait involves moving forward typically for more than one body length, planting one or more feet in contact with the ground, and then pulling on a load using a winch or similar mechanism. This mode of locomotion is typically slow, but has the advantage of a very long stroke length in comparison to body length. Therefore, any lost motion that is consumed in elastic deformation with each loading/unloading cycle is a small fraction of the overall work. While this mode does not allow momentum transfer across gait cycles, it does have the advantage of maintaining motion in a single cycle, thus pulling against kinetic friction more than static friction. Another way of achieving a uniform traction force with adhesion could be to employ adhesive belts, as demonstrated in some climbing robots [11], [12]. However, this solution introduces engineering challenges for steering while maintaining uniform adhesive pressure, which is important for maximum performance. The authors have found that they can obtain higher performance by bonding controllable adhesives to tiles that attach and release from the surface [22].

As shown in [4], small robots that utilize controllable adhesion in combination with a winch gait can pull loads many times their weight. In the next section we consider how to harness robots in teams for a larger combined load.

III. Considerations for Effective Load Sharing

We now consider the effect of gait on the ability to share loads. We seek to maximize the pulling capability of small teams of microrobots, with the aim of generating larger-than-human scale forces. Since we are interested in the case where the robots are much smaller than the load, the power output of the robots is necessarily small with respect to the load, and the load will be moved quasistatically. As a result, the metric we are primarily interested in is the peak force generated by the team of robots, rather than simply the power output or mean force. We assume that the robots will need to act against static friction, and momentum cannot be stored in the motion of the load.

We want to examine load sharing among N robots. We begin with the case of robots in parallel, with no effort taken to synchronize gaits. In this case, we assume that the time offsets between robot gaits are independently drawn from the uniform distribution from 0 to t_p. A representative time course of N robots is presented in Fig. 3a. This implies that the probability that a given robot is pulling at arbitrary time t^* is

$$p = t_c/t_p \tag{1}$$

Then the number of robots $n \leq N$ pulling together at an arbitrary time t^* follows the binomial distribution: $n \sim B(N,p)$. The total force follows the same distribution scaled by f_c.

The mean of a binomial distribution is always Np, meaning that the average force exerted by N robots is

$$F_{\text{mean}} = N f_c p \tag{2}$$

Analysis of the peak force is slightly more involved. We break this into two parts: estimating the effective number of

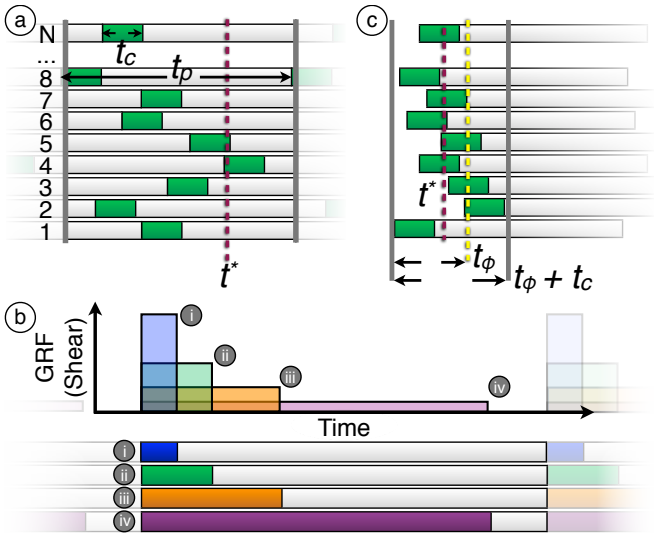

Fig. 3. (a) Uncoordinated pulling with N robots: Each robot takes strides of duration t_p, of which the foot is in contact for t_c. Phase delay between robots is assumed independent and uniformly random from 0 to t_p. (b) Example GRF of gaits of constant impulse demonstrating a range of cases from a sharp impulse at maximum frictional capacity: (i) $t_\mathrm{c}/t_\mathrm{p} = 0.085$, to the same body weight operating at nearly constant force (iv). (c) Coordinated pulling: phase delay is independent and uniformly random from 0 to t_ϕ, due to errors in synchronization.

robots acting together as a function of p, and estimating the peak force capability of a robot as a function of p.

Because the probability of all N robots pulling together quickly becomes negligible for small p or large N, we define an effective number of robots N_e to reflect the number of robots we expect to see pulling together some fraction of the time. Since the binomial distribution is only defined over integers in $[0, N]$, we define N_e as a linear interpolation to improve fit to measured data as follows:

Definition III.1. Let $c(x_1, N, p)$ be the cumulative distribution function of the binomial distribution $B(N, p)$ evaluated at integer $x_1 \in [0, N]$. Let $I(x_2, N, p)$ be a linearly interpolated CDF of B:

$$I(x_2, N, p) = c(\lfloor x_2 \rfloor, N, p) + \frac{x_2 - \lfloor x_2 \rfloor}{\lceil x_2 \rceil - \lfloor x_2 \rfloor} \cdot (c(\lceil x_2 \rceil, N, p) - c(\lfloor x_2 \rfloor, N, p)) \quad (3)$$

We then define $N_\mathrm{e}(N, p)$ as x such that $I(x, N, p) = 0.95$

This expression corresponds to the number of robots we expect to see pulling together 5% of the time from a team of N robots operating at p. Note that N_e is a function of N and p; for clarity, we simply note it as N_e; N and p where specified will be clear from context. We have found that interpolating between discrete values of the binomial distribution gives good results in practice.

For values of p near one, $N_\mathrm{e} \approx N$, i.e., the peak force produced by N robots is N times the peak force of one robot. As $p \to 0$, N_e approaches 0 monotonically, though N_e is less sensitive to p near 1. Depending on application, N_e could be defined with different percentiles to reflect how often the target peak force is required.

To model the force as a function of p, we first begin with the theoretical maximum. Since the robots have no net vertical acceleration, the average force they can exert is at most $\mu_\mathrm{e} mg$, where μ_e is the effective coefficient of friction, and mg is the weight. Given this time averaged force, a robot can exert a constant impulse per stride; varying t_c then gives differing peak forces, as seen in Fig. 3b.

The theoretical maximum is not achieved in practice, so we define a ground reaction force efficiency as

$$\eta_\mathrm{GRF} = \frac{f_\mathrm{c} p}{\mu_\mathrm{e} mg} \quad (4)$$

A robot has $\eta_\mathrm{GRF} < 1$; in general, η_GRF depends on p.

For modeling the force capabilities of a robot, we define a normalized force F_n as a function of p, normalizing the peak force by $\eta_\mathrm{GRF} \cdot \mu_\mathrm{e} mg$, which is the same as normalizing by the time-averaged force. This is a nondimensional measure representing force as a multiple of the robot's static capability, and is equal to 1 at $p = 1$ by definition.

Taken together, these results show that impulsive robots do not share load well, but make up for it by applying very high peak forces. Indeed, if we assume that a robot has constant impulse as p varies, then the model suggests that the robot should be as impulsive as possible to maximize peak force. Robots with a smooth gait will have t_c approaching t_p; in this case, all robots are likely to pull together, and $F \approx N \cdot f_\mathrm{c}$. Winched robots will only be pulling for a fraction of the stroke, and by the nature of the winching gait cannot exploit dynamics to increase peak force. Peak force remaining constant as p varies means that to maximize team efficiency p should be as large as possible. There is still a performance loss because p cannot be 1 for this gait.

However, winched robots tend to have longer step periods t_c, and this allows them to take advantage of in-phase pulling. Figure 3c shows a representative set of robots taking coordinated steps, slightly offset from each other. For simplicity we assume that this offset is uniform, following $U(0, t_\phi)$. With this upper bound, we know that all pulling strokes of the robots will occur within a window $t_\mathrm{c} + t_\phi$. The probability that any given robot is pulling at time t^* is

$$p = \frac{t_\mathrm{c}}{t_\mathrm{c} + t_\phi}. \quad (5)$$

So for synchronized robots, load sharing is effective when $t_\phi \ll t_\mathrm{c}$, and ineffective when t_ϕ is comparable to or larger than t_c. For winching robots, this is easily implemented due to the large step contact times, t_c. For more impulsive robots, synchronization becomes increasingly difficult, making load sharing less effective.

IV. Experiments

For experiments in load sharing we used several representative types of microrobots in different configurations. The first of these is Hexbug Nano, a commercially available toy bristlebot (Fig. 4a, *left*). The second is Hexbug Scarab, with silicone rubber added to the feet and tested with either 59 g or 32 g payload (Fig. 4a, *middle*). Varying the payload allows us

TABLE I
ROBOT AND OPERATION PARAMETERS

		Nano	Scarab Walking	Scarab Running	μTug
Gait		Impulsive	Smooth	Impulsive	Winch
Length	[mm]	43.9	54.8	54.8	28.6
Mass	[g]	7.65	78.1	49.0	17.7
Stride Frequency	[Hz]	27.8	2.9	16.9	0.015
Stride Length	[cm]	0.02	2.0	2.0	10
Peak Forward GRF	[N]	0.15	0.5	0.8	38
Mean Forward GRF	[N]	0.039	0.29	0.16	36
t_{p}	[s]	0.036	0.34	0.059	68
t_{c}	[s]	0.0071	0.23	0.010	65
η_{GRF}		0.04	0.9	0.8	0.9

to compare running and walking modes at a constant input power, with more weight resulting in a walking gait, and lighter weight in a running gait. The third type of microrobot is a μTug modified for increased actuator performance and durability (Fig. 4a, *right*). The relevant parameters of each of these configurations are summarized in Table I.

Other metrics commonly used to analyze gaits include the Froude number and the specific resistance [23]. However, these numbers are not particularly meaningful for the tested robots, which do not exhibit either a typical walking or trotting gait. The impulsive robots, like many other small robots that rely on friction, have substantial slippage, and the adhesive robots have an unusual gait with a long crawling "stride" followed by pulling with a winch. As a result, the most useful parameter for comparing the gaits is simply p, which is inversely correlated with Froude number.

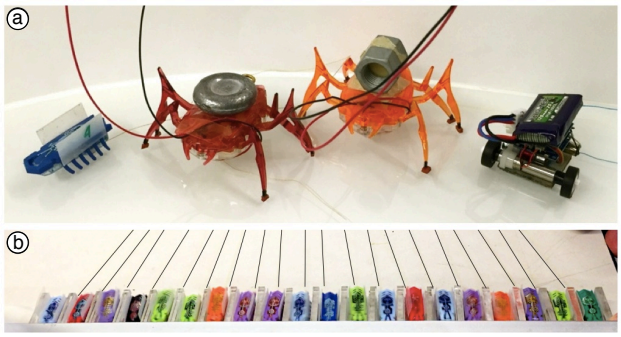

Fig. 4. (a) The four robots used in testing. From left, a Hexbug Nano, Hexbug Scarabs for walking and running, and a μTug. (b) Bristlebots in parallel. Load cell is out of frame towards the top, acrylic frame was used to constrain lateral motion. Tow lines are traced with black for contrast.

A. Methods

Force generation for Hexbug Nanos was measured by connecting the robots using a Kevlar tendon to an ATI Gamma F/T sensor sampled at 1 kHz. The robots were constrained laterally by placing them in corrals, with care to ensure minimal effect on forward force (Fig. 4b). The batteries were replaced for each test to ensure repeatable performance.

Both walking and running tests for the Hexbug Scarabs were conducted using the same basic framework. The robots were wired to external power supplies to enable gait adjustment for walking and running modes. Lateral motion was constrained using a pair of parallel plastic rails protruding between the robot legs and body. The rails were spaced far enough to ensure the robots didn't bind and, as with the Nanos, the friction in the pulling direction was negligible with respect to the measured force. Out of the box, the Scarabs walk with an alternating tripod gait using hard plastic feet. These were modified by adding silicone rubber pads, to increase the coefficient of friction ($\mu_{\mathrm{k}} \approx 0.4$).

For both sets of tests, we used two metrics to describe the force profiles: the mean force, taken as the average force during the test; and the peak force, which we defined as the force at the 95th percentile of all local peaks during the test. This latter measurement represents the magnitude of the peak force that is expected to occur relatively often, rather than the measurement of the single best peak, which is likely an outlier.

The μTugs were tested on a glass surface using a strain gauge load sensor on each robot to measure pulling forces. Data were sampled at 125 Hz using a Phidgets 20 kg Micro Load Cell and a PhidgetsBridge. Each μTug was powered using a separate DC power supply to allow for tuning of the robots' force output. The duty cycle to each robot was controlled using MOSFETs controlled from a common signal to maintain synchronization. The mean force was defined as the mean force applied during a pull. The peak force is the mean value of peaks greater than 0.1 s wide during the pull.

V. RESULTS

Fig. 5 shows for each robot type: GRF measurements, total peak team force, and force per robot. For total team force, model fits using the model described in Sec. III are presented as dotted lines. For the impulsive, walking, and running robots, $f_c p$ was estimated as the time-averaged force per robot when testing the maximum number of robots. The fraction of time spent applying an impulse, p, was calculated by finding the fraction of time spent above half-maximum of the peak force. This force level is shown in the first row of Fig. 5 as dashed lines. The μTugs were run in synchronization, and p was calculated using measured values of t_{c} and t_{ϕ}. The model-predicted force output is plotted alongside measured data in the second row as dotted lines. The individual results will be examined in the following subsections.

A. Impulse Driven Bristlebots

Bristlebots tested in parallel (Fig. 5, *column a*) demonstrated the basic relationship between peak force and subsequent additional force expected by the model. As shown in (*i*), the robot ground reaction force is highly impulsive. Hence the peak pulling force for a single robot can be high—in this case 0.15 N, representing a force about twice its weight. Subsequent robots added substantially less additional peak force—an average of 0.03 N or about half a body weight each, over the next 19 robots. The model estimates that 20 robots will generate 0.9 N of force, 20% greater than the

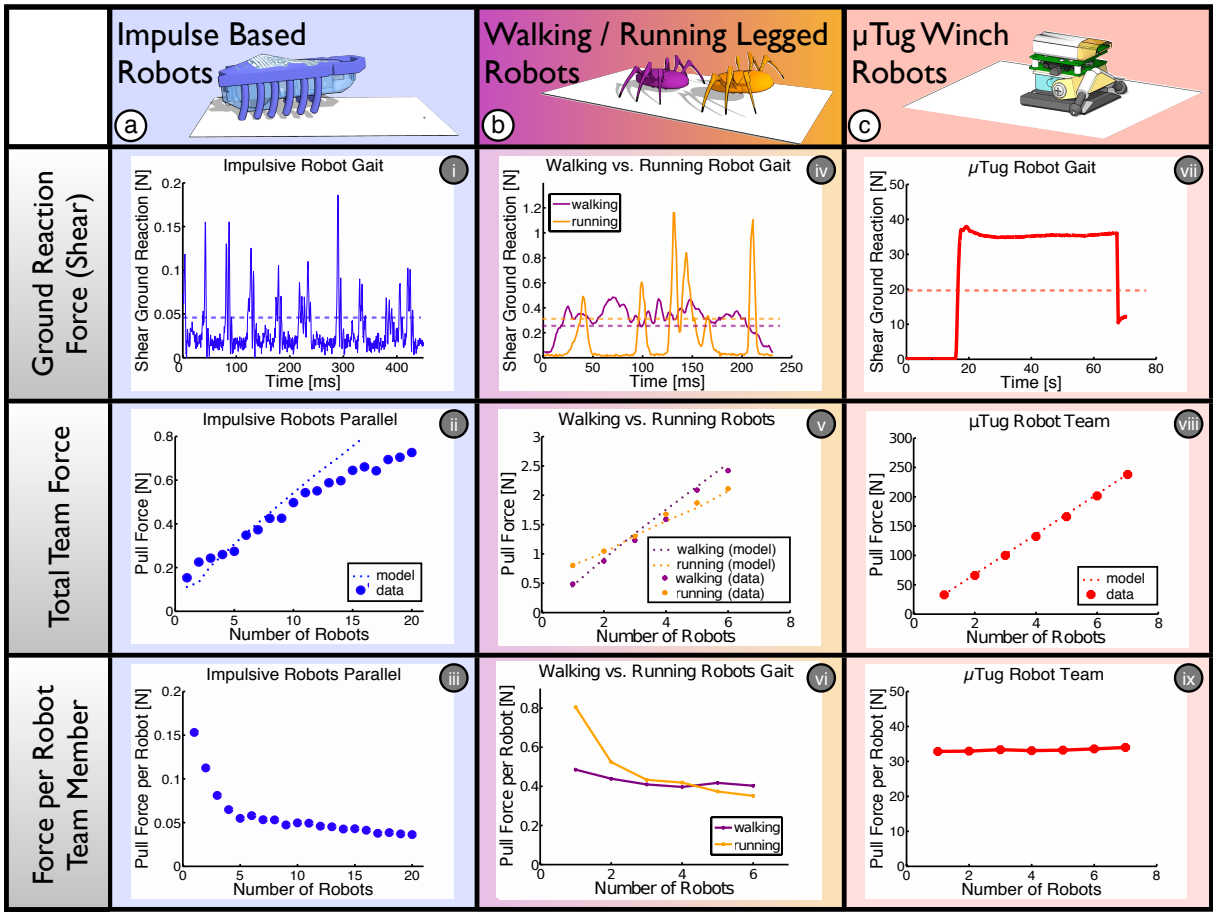

Fig. 5. Combined data for the 3 different robots tested. *Column a*: Bristlebot impulse robots. *Column b*: 6 legged robots walking and running. *Column c*: Winch gait µTugs. The first row (*i*,*iv*,*vii*) is representative GRF data for each condition, the second (*ii*,*v*,*viii*) shows the 95th percentile force as a function of robots in the team, and the third row (*iii*,*vi*,*ix*) shows the same force data normalized by number of robots. Note the trends in *v*: for single robots, running provides greater peak force, but as the number of robots increases, walking robots surpass them with superior load sharing.

observed $0.75\,\mathrm{N}$. This is reasonably accurate, given that we expect the model to over-predict performance for impulsive forces; the flat force profile assumed in the model becomes increasingly unrepresentative of the true force.

For comparison, smoothly moving robots of equal weight and frictional properties could have contributed up to $0.9\,\mathrm{N}$ each. This means that the impulsive bristlebots only have an efficiency η_{GRF} of about 0.04. The high-speed video included in the media file shows why: each robot is mainly hopping up and down with only a slight forward bias and never makes full use of the available friction.

One way to improve load sharing is to synchronize the impulses. This was done using a voice coil actuator to seismically excite the robots on a rigid plate. However, this reasonable effort at synchronization was not any better than the unsynchronized case. This is largely because of the variability of bounce heights; a difference of only $0.5\,\mathrm{mm}$ corresponds to a difference of time in the air of $0.01\,\mathrm{s}$, or about 5 times t_{c}, which is not tight enough to improve performance.

As a rough estimate, it would take over 4000 bristlebots hooked up in parallel to pull a car. This number of robots is so large that it exceeds the available perimeter of the car. A convenient alternative way to exert large forces would be to arrange some robots in series; data comparing series and parallel performance are presented in Fig. 6.

The first robot in the series test again provides $0.14\,\mathrm{N}$, but in this case the subsequent 19 robots only provide a vanishingly small average additional force of $0.008\,\mathrm{N}$ per robot. This trend is generally seen whenever extra mass is in the force path, which produces the effect of attenuating sharp force transients. Similar effects would be seen for tendons of finite stiffness absorbing cyclic energy, as well as non-rigid loads consisting of spring-mass networks.

B. Legged Robots Walking or Running

Unlike the bristlebots, the legged robots present an opportunity to observe the effects of varying gait. By driving the motor to make the feet slip when pulling under the robot's own weight, the robots can achieve a smooth walking gait. Extra weights were added ($56\,\mathrm{g}$) to keep a consistent gait that did not stall. By fixing the power used by the motors, but reducing the added weight, we make the same robots shift to a running gait. This gait has the same robot kinematics, but is fast enough that the feet leave the ground, bouncing and running similarly to many running robots [6], [24], [25].

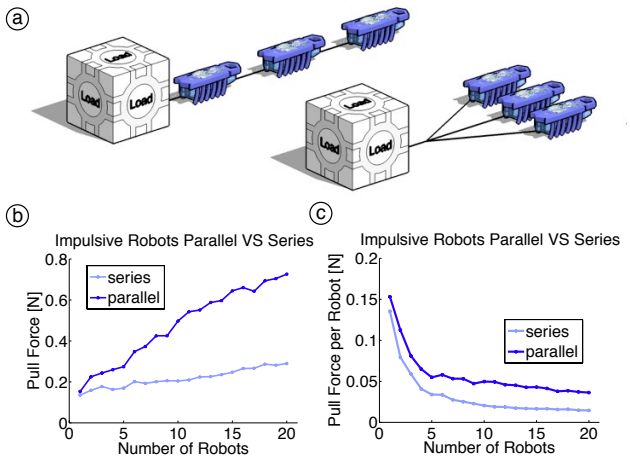

Fig. 6. (a) Two different pulling conditions for bristlebot: robots in series are attached to a single tendon, connected to the load; robots in parallel have individual tendons that merge at the load. (b) Peak force output with increasing numbers of robots for parallel and series cases. (c) Force per robot for parallel and series cases, indicating that additional robots contribute less extra capability.

The robots in both these operating conditions were much better than the nano bristlebots at using the available friction (η_{GRF} of 0.9 and 0.8 for walking and running respectively). However, as seen in Fig. 5(*iv*), they had very different ground reaction forces in the two gaits. Running is impulsive, while walking is much smoother.

In both cases, the robots have similar normalized force curves $F_{\mathrm{n}}(p)$. The running robots have an initially higher peak force corresponding to a high enough normalized force to offset the weight difference. However, the load sharing effectiveness becomes important as more robots are added. As seen in Fig. 7, as p decreases, the load sharing decreases significantly. This results in the behavior shown in Fig. 5(*v*); the walking robots have better load sharing, and soon overtake the running robots in terms of peak performance.

While here we fixed power and varied mass, if the opposite is done the model predicts that running will always have higher peak forces. This result was confirmed in practice for up to five robots. Critically, this does not take into account the large increase in power required to achieve such a gait.

C. Winching μTugs

The μTugs presented in [4] used gecko-inspired adhesives to apply human scale loads. The robots are constructed with a single flat foot to maximize contact area and therefore adhesive capability. The result is a gait consisting of a sequence of long static winch pulls with uniform force, followed by forward motion or steering as the winch unwinds. The time scales of this gait make synchronization much easier than for the impulsive robots, and p of nearly unity can be achieved using any sort of inter-robot communication or coordination.

When the high pulling force of the μTugs is combined with load sharing, a team of seven can provide a peak force of 375 N (85 lbf) in shear (Fig. 8).

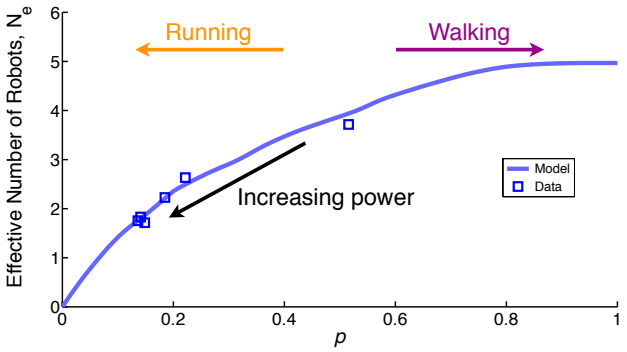

Fig. 7. Model and experimental results for load sharing among five legged robots varied from walking to running gaits. Normalizing the measured force by the force from a single robot allows us to isolate the effect of load sharing irrespective of force capability. By varying the power input by a factor of 4, the robots operate at p from 0.52 to 0.14.

D. Active Load Sharing

As demonstrated in [26], one of the biggest challenges in making efficient use of an adhesive system is loading the adhesive up to but not over its limit. While there are several passive options that equally distribute force, they are all limited by the weakest element in the set. Even worse, some require an estimate of the weakest element's long term performance on any surface at the time of construction. Having each tile equipped with feedback and an independent actuator can avoid these problems.

To get the peak value of 375 N shown in Fig. 8 each robot was placed on glass and independently loaded by increasing the motor drive voltage until adhesive slipping occurred. When testing in concert, each robot is controlled to exert its individual maximum force so that the total force is more than seven times that of the weakest team member. Indeed, the sum of the peak values measured at any time through the test is nearly equal to the sum of the independently measured peak results.

VI. Discussion: Model Insights

Before we discuss predictions from the statistical model, we first look at the fit between model and measured data. Fig. 5(*ii*,*v*,*viii*) show the predicted load sharing forces for the tested number of robots of each type. The fit in (*v*) and (*viii*) is very good, and as previously noted, the fit in (*ii*) is overpredicting the results as expected due to the sharpness of the impulsive spikes.

A closer look at the legged robots as they move from walking to running gaits provides more insight into how these robots interact as a team. Fig. 7 shows the expected load sharing in terms of N_{e} for five robots as p changes. To obtain these data, total force from a team of five robots was measured at different values of p. The force capabilities of a single robot were also measured at the same values of p. Fig. 7 therefore plots team force capability independent of individual robot performance.

There is a good match in this test for p from 0.52 to 0.14. The model therefore gives us a good idea of how load sharing is affected by p: load sharing performance decreases

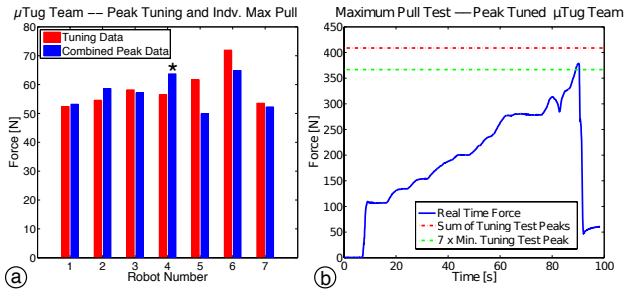

Fig. 8. Tuning data and results for a team of 7 μTugs. (a) Individual force capability of each robot (red) and the peak measured force during the team test (blue). Due to the open loop control, robot 4 (starred) exceeded its capability and ended the test by slipping. (b) Combined force of the team, with the maximum force possible with a passive system in green, and theoretical active load sharing limit in red. Note that measured force exceeds the theoretical limit of a passive system.

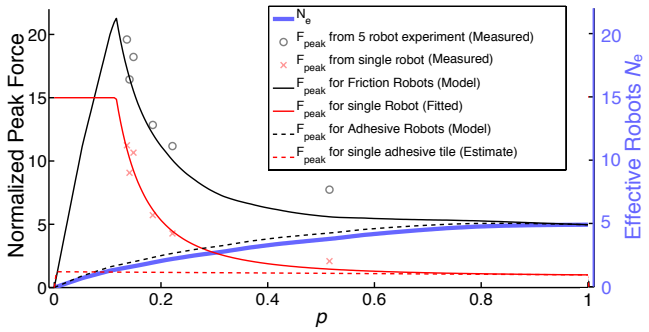

Fig. 9. *Solid blue,* N_e: as in Fig. 7, the effective number of robots in a load sharing team, for $N = 5$, as a function of p. Combining this with individual robot normalized forces, we predict the force capability of robot teams: *solid red* is the normalized force, F_n, for a single legged robot as p varies; red crosses show data used to fit F_n. Multiplying F_n by the number of effective robots, N_e, gives the predicted normalized force from a team of 5 legged robots (*solid black*); gray circles show corresponding measured values. *Dashed red* is the normalized force, F_n, for a single μTug . Scaling by N_e yields (*dashed black*) predicted force from 5 μTugs. Because the shape of F_n is different in the two cases, optimum value of p for the μTug is close to 1.

as p decreases. All else being equal, operating at lower p means that on average fewer robots are doing useful work at a given time.

We now address the normalized force component of the model. Fig. 9 includes a fit of the normalized force, F_n, generated by a single legged robot. In this case, data were taken for single robots, and normalized by the friction-limited steady force capability, $\mu_e mg$. These normalized data are plotted as red crosses, and were used to fit F_n. The fitting function (solid red) has the form $c_1/p^{c_2}+(1-c_1)$, and is thus defined to be 1 at $p = 1$; this is a known point representing a steady force using kinetic friction. While we expect constant-impulse force to vary as $1/p$, we allow the power of p to vary to obtain a better fit to the measured data. The impulse of the fitted force profile is very close to constant, but this also predicts that the force diverges to infinity as p approaches 0. Since we know the robot will break before applying infinite force we cap its force capabilities at 10% over the peak experimentally measured force, apparent for $p \leq 0.1$.

Plotting the product $N_e F_n$ with respect to p gives the normalized performance of a team of robots. In Fig. 9, this is the solid black curve. Also plotted are the same experimental data presented in Fig. 7, but normalized by steady-state force, not force at the operating p (gray circles). These data, which are measured for five robots, closely match the force predicted by the model from measurements of one robot.

Conveniently, with frictional walking robots, power can be traded for speed, permitting a wide range of p values from 0.52 to 0.14 and thus extra individual capability. In this particular case, the gain outweighs the loss in load sharing, and the peak team force occurs when the robots are operated near the break point of the force profile.

In general, the best p for peak load depends on the shape of the normalized force curve. When combined with the statistical model for load sharing, a given team size will have a resulting capability depending on p. For a given task with a minimum force requirement, the team will either be incapable of performing the task, or there will be a region of feasible p. Within this region, one can optimize for other constraints. In the case of these walking robots with a high power cost associated with making more impulsive forces, the team will likely be optimized to maximize p while still achieving the minimum force, maximizing team efficiency.

This example changes dramatically when we consider the adhesives used by the μTugs. Unlike the frictional case, the behavior of the adhesive does not allow dynamic boosting of the maximum force capability, and in fact will not adhere for $t_c < 5$ ms. The resulting normalized force curve is nearly flat through the entire range of p. As seen in Fig. 9, the maximum peak capability occurs essentially at $p = 1$.

Together, these trends suggest a design procedure for robot teams. Having determined the required force for a task, robots can either be added to the system, or tuned for improved peak force. The result is a set of feasible team configurations whose performance can be predicted via use of the model and characterization of a single robot. The system can be optimized within the set of feasible configurations for cost, efficiency, speed, etc.

VII. Conclusions and Future Work

When combining small robots in teams to pull large loads, it is important to consider the details of their ground reaction forces. For robots with a smooth gait, the result of adding robots is straightforward, especially for the quasistatic loads explored. However, for robots with an impulsive gait, the picture is more complicated. The performance of the legged robots walking and running reveals a crossover in performance; the best single robot in terms of peak force capability is not necessarily the best robot to use in a team.

While it was not within the scope of this paper, we note that for many payloads, the use of impulsive robots requires that one must consider the dynamics of the load as well, including impedance matching, etc.

The developed statistical model shows good results in predicting the behavior of teams of robots within measurement noise and is reasonably accurate for both impulsive and smooth robot gaits. Although the assumptions made in

the model are less valid for highly impulsive robots, the results of experiments are predicted well enough for at least a qualitative understanding of the phenomena involved. For microrobots much smaller than those tested, the details of their dynamics and ground interactions will be different. However, the statistical model is independent of such details, as it depends only on contact duration versus stride length.

A basic design methodology was suggested for designing teams of robots based on trading off peak force and gait smoothness versus the number of required robots for a given set of task requirements. These principles were applied to make a team of µTugs capable of pulling a 1800 kg automobile, while crawling on polished concrete.

A. Future work

Although the adhesive force profile is not highly dependent on the loading rate, careful use of the adhesive can yield up to a 25% boost in peak force capability. Future work will include rapidly-loaded adhesive robots that exploit this effect, and using active sensing [27] to monitor and control the force applied by each robot in a team, increasing robustness on imperfect surfaces.

ACKNOWLEDGMENT

The authors thank their families and friends for support and encouragement as well as S. Christensen, H. Jiang, E. Hawkes, E. Eason, and T. Kenny for their aid. This work was partly supported by DARPA under Contract HR0011-12-C-0040; any opinions, findings or recommendations are those of the authors and do not necessarily reflect the views of DARPA. Additional support was provided by NSF IIS-1161679 and ARL MAST MCE14-4.

REFERENCES

[1] J. Sudd, "The transport of prey by ants," *Behaviour*, vol. 25, no. 3, pp. 234–271, 1965.

[2] C. R. Kube and E. Bonabeau, "Cooperative transport by ants and robots," *Robotics and autonomous systems*, vol. 30, no. 1, pp. 85–101, 2000.

[3] S. Berman, Q. Lindsey, M. S. Sakar, V. Kumar, and S. Pratt, "Study of group food retrieval by ants as a model for multi-robot collective transport strategies." in *Robotics: Science and Systems*, 2010.

[4] D. Christensen, E. Hawkes, S. Suresh, K. Ladenheim, and M. Cutkosky, "μTugs: Enabling microrobots to deliver macro forces with controllable adhesives," in *IEEE ICRA*, May 2015, pp. 4048–4055.

[5] I. Paprotny and S. Bergbreiter, "Small-scale robotics : An introduction," in *Small-Scale Robotics. From Nano-to-Millimeter-Sized Robotic Systems and Applications*, ser. Lecture Notes in Computer Science, I. Paprotny and S. Bergbreiter, Eds. Springer Berlin Heidelberg, 2014, vol. 8336, pp. 1–15.

[6] A. T. Baisch and R. J. Wood, "Pop-up assembly of a quadrupedal ambulatory microrobot," in *IROS*. IEEE/RSJ, 2013, pp. 1518–1524.

[7] Y. Han, H. Marvi, and M. Sitti, "Fiberbot: A miniature crawling robot using a directional fibrillar pad," in *ICRA*. IEEE, 2015, pp. 3122–3127.

[8] X. Zhou, C. Majidi, and O. OReilly, "Energy efficiency in friction-based locomotion mechanisms for soft and hard robots: slower can be faster," *Nonlinear Dynamics*, vol. 78, no. 4, pp. 2811–2821, 2014.

[9] B. R. Donald, C. G. Levey, and I. Paprotny, "Planar microassembly by parallel actuation of mems microrobots," *Microelectromechanical Systems, J. of*, vol. 17, no. 4, pp. 789–808, 2008.

[10] B. Seitz, B. Goldberg, N. Doshi, O. Ozcan, D. Christensen, E. Hawkes, M. Cutkosky, and R. Wood, "Bio-inspired mechanisms for inclined locomotion in a legged insect-scale robot," in *ROBIO*. IEEE, 2014, pp. 791–796.

[11] M. Greuter, G. Shah, G. Caprari, F. Tâche, R. Siegwart, and M. Sitti, "Toward micro wall-climbing robots using biomimetic fibrillar adhesives," in *3rd Intl. Symposium on Autonomous Minirobots for Research and Edutainment (AMiRE 2005)*. Springer, 2006, pp. 39–46.

[12] J. Krahn, Y. Liu, A. Sadeghi, and C. Menon, "A tailless timing belt climbing platform utilizing dry adhesives with mushroom caps," *Smart Materials and Structures*, vol. 20, no. 11, p. 115021, 2011.

[13] E. Hawkes, D. Christensen, and M. Cutkosky, "Vertical dry adhesive climbing with a 100x; bodyweight payload," in *ICRA*. IEEE, 2015, pp. 3762–3769.

[14] M. Rubenstein, C. Ahler, and R. Nagpal, "Kilobot: A low cost scalable robot system for collective behaviors," in *ICRA*. IEEE, 2012, pp. 3293–3298.

[15] A. Becker, G. Habibi, J. Werfel, M. Rubenstein, and J. McLurkin, "Massive uniform manipulation: Controlling large populations of simple robots with a common input signal," in *IROS*. IEEE/RSJ, 2013, pp. 520–527.

[16] E. Diller, C. Pawashe, S. Floyd, and M. Sitti, "Assembly and disassembly of magnetic mobile micro-robots towards deterministic 2-d reconfigurable micro-systems," *IJRR*, pp. 1667–1680, 2011.

[17] S. Seok, A. Wang, M. Y. Chuah, D. Otten, J. Lang, and S. Kim, "Design principles for highly efficient quadrupeds and implementation on the mit cheetah robot," in *ICRA*. IEEE, 2013, pp. 3307–3312.

[18] D. R. Frutiger, K. Vollmers, B. E. Kratochvil, and B. J. Nelson, "Small, fast, and under control: wireless resonant magnetic micro-agents," *IJRR*, vol. 29, no. 5, pp. 613–636, 2010.

[19] D. L. Christensen, E. W. Hawkes, A. Wong-Foy, R. E. Pelrine, and M. R. Cutkosky, "Incremental inspection for microrobotic quality assurance," in *IDETC/CIE*. ASME, 2013.

[20] R. J. Full and M. S. Tu, "Mechanics of a rapid running insect: two-, four-and six-legged locomotion," *J. of Experimental Biology*, vol. 156, no. 1, pp. 215–231, 1991.

[21] "Castrillo_de_Villavega_Festival_of_La_Trilla_Plowing_004.jpg" by Valdavia is used under CC. Desaturated from original, Accessed: 2015-08-30.

[22] E. W. Hawkes, E. V. Eason, A. T. Asbeck, and M. R. Cutkosky, "The geckos toe: scaling directional adhesives for climbing applications," *Mechatronics, IEEE/ASME Transactions on*, vol. 18, no. 2, pp. 518–526, 2013.

[23] R. M. Alexander, "Energy-saving mechanisms in walking and running," *J. of Experimental Biology*, vol. 160, no. 1, pp. 55–69, 1991.

[24] P. Birkmeyer, K. Peterson, and R. S. Fearing, "Dash: A dynamic 16g hexapedal robot," in *IROS*. IEEE/RSJ, 2009, pp. 2683–2689.

[25] D. W. Haldane, K. C. Peterson, F. L. Garcia Bermudez, and R. S. Fearing, "Animal-inspired design and aerodynamic stabilization of a hexapedal millirobot," in *ICRA*. IEEE, 2013, pp. 3279–3286.

[26] E. W. Hawkes, E. V. Eason, D. L. Christensen, and M. R. Cutkosky, "Human climbing with efficiently scaled gecko-inspired dry adhesives," *J. of The Royal Society Interface*, vol. 12, no. 102, p. 20140675, 2015.

[27] X. A. Wu, S. A. Suresh, H. Jiang, J. V. Ulmen, E. W. Hawkes, D. L. Christensen, and M. R. Cutkosky, "Tactile sensing for gecko-inspired adhesion," in *IROS*. IEEE/RSJ, 2015.